

Reprinted from

JAPANESE JOURNAL OF
**APPLIED
PHYSICS**

SELECTED TOPICS IN APPLIED PHYSICS

**Cooper-Pair Radiative Recombination in Semiconductor Heterostructures:
Impact on Quantum Optics and Optoelectronics**

Ikuo Suemune, Hirotaka Sasakura, Yujiro Hayashi, Kazunori Tanaka, Tatsushi Akazaki,
Yasuhiro Asano, Ryotaro Inoue, Hideaki Takayanagi, Eiichi Hanamura, Jae-Hoon Huh, Claus Hermannstädter,
Satoru Odashima, and Hidekazu Kumano

Jpn. J. Appl. Phys. **51** (2012) 010114

Cooper-Pair Radiative Recombination in Semiconductor Heterostructures: Impact on Quantum Optics and Optoelectronics

Ikuo Suemune^{1,2*}, Hiroataka Sasakura^{1,2}, Yujiro Hayashi¹, Kazunori Tanaka^{2,3}, Tatsushi Akazaki^{2,4}, Yasuhiro Asano⁵, Ryotaro Inoue^{2,6}, Hideaki Takayanagi^{2,6,7}, Eiichi Hanamura⁸, Jae-Hoon Huh^{1,2}, Claus Hermannstädter¹, Satoru Odashima^{1,9}, and Hidekazu Kumano^{1,2}

¹Research Institute for Electronic Science, Hokkaido University, Sapporo 001-0020, Japan

²CREST, Japan Science and Technology Agency, Kawaguchi, Saitama 332-0012, Japan

³Central Research Laboratory, Hamamatsu Photonics, Hamamatsu 434-8601, Japan

⁴NTT Basic Research Laboratories, Atsugi, Kanagawa 243-0198, Japan

⁵Graduate School of Engineering, Hokkaido University, Sapporo 060-8628, Japan

⁶Department of Applied Physics, Tokyo University of Science, Shinjuku, Tokyo 162-8601, Japan

⁷International Center for Materials Nanoarchitectonics, NIMS, Tsukuba, Ibaraki 305-0044, Japan

⁸Japan Science and Technology Agency, Kawaguchi, Saitama 332-0012, Japan

⁹GCOE, Graduate School of Information Science and Technology, Hokkaido University, Sapporo 060-0814, Japan

Received June 30, 2011; accepted September 6, 2011; published online December 6, 2011

The injection of Cooper pairs into a normal medium such as a semiconductor is known as the proximity effect at the superconductor/normal interface. We confirm this injection as well as the contribution of Cooper pairs to a drastic enhancement of inter-band optical transitions in semiconductor heterostructures. In this paper we investigate and clarify the relation of internal quantum efficiencies and radiative lifetimes in Cooper-pair light emitting diodes (CP-LEDs). A quantitative description of the dynamic photon generation processes is given, and the contribution of the Cooper-pair recombination relative to normal-electron recombination in CP-LEDs is discussed in detail.

© 2012 The Japan Society of Applied Physics

1. Introduction

Superconductivity is expanding its global position because of the scientific and technological importance. Quantum information processing is one potential application field with superconducting qubits as promising candidates as the basic elements/building blocks in such devices.¹⁻⁴ As another example, quantum cryptography is believed to approach the stage of practical application,⁵⁻⁸ and furthermore, the expansion to more complex quantum information networks based on photon qubits is expected. For such an expansion, a reliable conversion from superconducting qubits to “flying” photon qubits and *vice versa* is an essential requirement for the connection of information-processing and transfer. Quantum gates based on the manipulation of superconducting qubits with low energy photons, such as microwaves, have been actively studied and demonstrated.¹⁻⁴ However, the interaction of superconducting states with photons for optical-fiber communication has been much less studied due to the lack of basic interdisciplinary technologies connecting superconductivity and optoelectronics.

In the field of quantum optics, entangled photon pairs (EPPs) are getting more and more important for quantum information processing and communication. As a principal protocol of quantum key distribution (QKD) for quantum cryptography, an entanglement-based protocol called BBM92⁹ and related applications¹⁰ have been proposed in addition to single-photon-based protocols such as BB84.¹¹ Quantum teleportation was proposed by Bennett¹² and was demonstrated employing EPPs.¹³ EPPs employed for these experiments were generated with parametric down conversion (PDC),¹⁴ which became a standard method in the related fields. Lasers are generally used as sources for PDC and the directionality of the generated EPPs facilitates the application of EPPs to relevant purposes. However

the coherence of the excitation laser sources results in a Poissonian statistics of the generated photon number states,¹⁵ which is why the generation sequence of EPPs cannot be regulated. This drawback has triggered the research toward “on-demand operation” of regulated EPP sources. To date, mainly semiconductor quantum dot (QD) based sources have been extensively studied.¹⁶⁻¹⁹ The main scheme to generate EPPs from QDs is the cascaded recombination process of biexcitons and excitons which results in the emission of photon pairs with a time separation (delay) on the order of 1 ns, which is determined by the exciton lifetime.^{16,17}

The possibility of simultaneously generating EPPs from semiconductors has been demonstrated with parametric scattering of biexciton polaritons in CuCl.^{20,21} However, the excitation source is a laser, resulting again in a Poissonian distribution of the generated EPPs. In semiconductors the two-photon absorption process is well known, which is the second-order process of simultaneous absorption of two photons with photon energies of half the energy gap each. The generation of EPPs with a two-photon emission process, which is the reverse process of two-photon absorption, has been demonstrated employing a GaInP/AlGaInP waveguide.²² This is a spontaneous generation process of EPPs and is thus not suffering the aforementioned Poisson statistics issue. The remaining problem is that the first-order process of single-photon generation dominates the recombination process, and thus the two-photon emission probability is comparably low — on the order of 10^{-5} of the one-photon process.²²

We have proposed another possibility to generate EPPs employing Cooper-pair radiative recombination processes.^{23,24} This new possibility of involving Cooper pairs in the photon generation process is also a step toward developing basic technologies to connect superconducting and photon qubits. The role of Cooper pairs in radiative recombination processes has been demonstrated with

*E-mail address: isuemune@es.hokudai.ac.jp

Cooper-pair injection from niobium (Nb) superconducting electrodes into an InGaAs light emitting diode (LED).²⁵⁾ Drastic enhancement of electroluminescence (EL) output was observed below the Nb superconducting critical temperature (T_C). This phenomenon was theoretically explained by a Cooper-pair recombination with a pair of normal holes, which leads to a simultaneous generation of one EPP.²⁶⁾ The essential role of Cooper-pairs is found in the enhancement of radiative recombination via the condensation of electrons near the Fermi level into superconducting states. This enhancement was directly observed via the reduction of the radiative lifetime below Nb T_C .²⁷⁾ The EL enhancement, which indicates the enhancement of the internal quantum efficiency (IQE), and the reduction of radiative lifetimes (or enhancement of radiative recombination rates) are correlated with one another. However the mutual relations given in the previous reports^{25,27)} are quite different and apparently not simple.

In this paper the relation of IQE and radiative lifetimes is formulated from a general viewpoint, and the mutual relation of the previous reports and the role of Cooper pairs in both circumstances are clarified. The transient photon emission processes are apparently more involved with additional factors; consequently, a fundamental formulation dealing with the transient response is given which makes a self-consistent interpretation of our observations possible. Based on these analyses, the Cooper-pair recombination process relative to the normal recombination process in the LED operation is quantitatively evaluated.

2. Fundamental Scheme of Cooper-Pair LED and Cooper-Pair Injection

The fundamental band diagram of the proposed Cooper-pair LED (CP-LED) is shown in Fig. 1. It is a conventional p-i-n heterostructure except for the Cooper-pair injection into the central active layer. In this diagram the electron Cooper-pair injection is assumed from a superconducting electrode formed on the n-type semiconductor surface. The Cooper-pair injection at the superconductor-semiconductor (S-Sm) junction is known as the proximity effect.²⁸⁾ The key issue is the Cooper-pair penetration into the active layer without energy relaxation at the n-type barrier/active layer hetero-interface.²⁴⁾ Injected Cooper pairs recombine with a pair of holes which are injected from the counter-side p-type barrier through a normal metal electrode and are expected to generate EPPs simultaneously.

The top view of a typical CP-LED device is shown in Fig. 2(a). The employed semiconductor is an n-type InGaAs heterostructure [a 10-nm-thick n-In_{0.7}Ga_{0.3}As contact layer, a 20-nm-thick n-In_{0.53}Ga_{0.47} barrier layer, and a 10-nm-thick n-In_{0.6}Ga_{0.4}As quantum well (QW) layer in ref. 25; the QW layer was replaced with a 10-nm-thick n-In_{0.53}Ga_{0.47} barrier layer in ref. 27] grown on a p-type InP substrate as shown in Fig. 2(c), whose surface is covered with a SiN insulating layer. The Nb electrode is formed in “H shape” and is connected with four gold (Au) pads. The pairwise arrangement of Au pads on the left (right) side is for the purpose of measuring Nb T_C , and a narrow slit is formed at the center of the Nb electrode as shown in the expanded view [Fig. 2(b)]. This part of the Nb electrode is in direct contact with the n-InGaAs surface, where the contact area is either

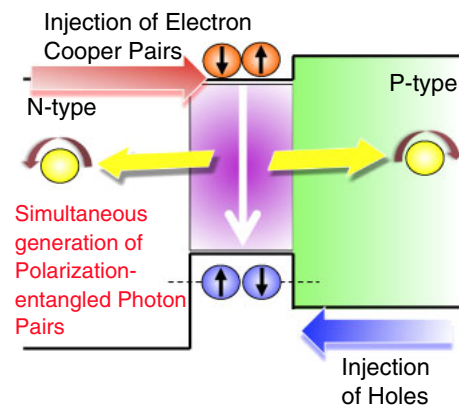


Fig. 1. (Color online) Fundamental band diagram and operation principle of a CP-LED.

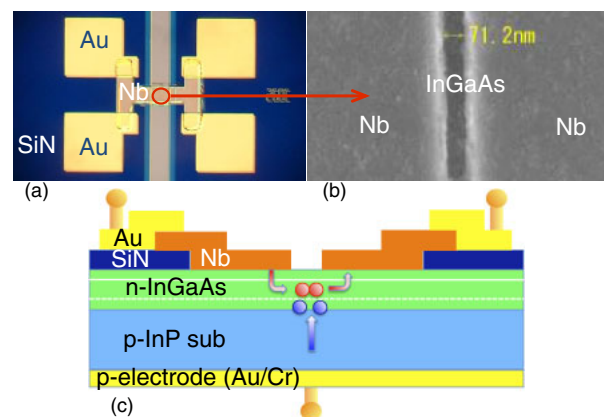


Fig. 2. (Color online) (a) Top view of a typical CP-LED structure. (b) Its expansion around the slit formed in the Nb electrode. (c) Cross-sectional view of the CP-LED. Electron Cooper-pair injection from the Nb electrodes into the n-InGaAs and recombination with a pair of holes injected from the p-electrode through the p-InP substrate is schematically shown.

$50 \times 50 \mu\text{m}^2$ (ref. 25) or $20 \times 40 \mu\text{m}^2$ (ref. 27) which is defined by the SiN insulating mask.

The injection of electron Cooper pairs into the InGaAs semiconductor is examined by measuring the current-voltage (I - V) characteristics through the S-Sm-S junction defined by the Nb slit. Details of the measurements are reported in ref. 29, but one example of the observed Josephson junction property is shown in Fig. 3. This data was measured on the sample with a slit width of 110 nm and the critical supercurrent was $\sim 1 \mu\text{A}$ at the extremely low temperature of 30 mK.³⁰⁾ Our recent developments of Nb nano-patterning technology allow reducing the Nb slit width down to 20 nm.³¹⁾ With a slit width of only 80 nm, an increased critical supercurrent up to $50 \mu\text{A}$ was observed for temperatures below 1 K and the Josephson junction property was observable up to almost T_C of 8.7 K.³¹⁾

In addition to these DC Josephson junction characteristics, electron Cooper pair injection was confirmed with measurements of the AC Josephson effect. By irradiating microwaves, voltage steps (usually called Shapiro steps) were observed in the I - V characteristics³²⁾ with the incremental voltage step ΔV proportional to the irradiated frequency

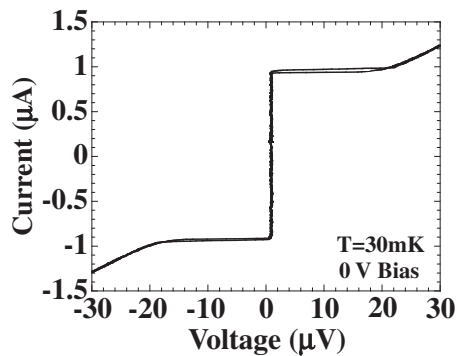


Fig. 3. I - V characteristic measured through the S-Sm-S junction (width of 20 μm) formed on the surface of a CP-LED.

f according to the following relation, $\Delta V/f = h/2e = 2.1 \mu\text{V}/\text{GHz}$, where h is the Plank constant and e is the electron charge. These steps occur due to the absorption of microwave photons by Cooper pairs and are another evidence of Cooper pair injection into the InGaAs semiconductor.

In the following paragraph, the reason why InGaAs is selected for the CP-LED is discussed. According to the Blonder-Tinkham-Klapwijk (BTK) theory,³³⁾ the supercurrent through a S-N junction is sensitively dependent on the tunnel barrier at the interface. In this simple model, a delta-functional barrier with the barrier height of Z was assumed and the results were critically dependent on the value of Z . In our experiments, the S-Sm junction barrier height corresponding to Z is the Schottky barrier at the metal-semiconductor interface. The conduction-band barrier height at metal/n-In_xGa_{1-x}As interface is given by $\Delta E_C = 0.95 - 1.90x + 0.90x^2$ (eV)³⁴⁾ and nonalloyed Ohmic contacts are possible for $x \sim 0.8$. This makes reproducible Cooper-pair injection into the n-InGaAs possible. The Schottky barrier height at Nb/p-InGaAs is much higher. Hole Cooper-pair injection is still possible;³⁵⁾ however, in this case the critical supercurrent is one order of magnitude lower than that in the Nb/n-InGaAs case with electron Cooper pairs.²⁴⁾

The above observations demonstrate that electron Cooper-pairs are successfully injected and flow in the n-InGaAs layers through the S-Sm-S junction formed on the CP-LED surface. Since this device has three terminals including the two n-type electrodes and a back p-type electrode, it operates as a junction field-effect transistor (J-FET) at room temperature.³⁶⁾ Reverse bias on the back p-type (gate) electrode increases the depletion layer width at the p-n junction (p-InP and n-InGaAs heterojunction) and reduces the n-type channel width for the electron transport in the n-InGaAs layer. Moderate forward bias of the back gate cancels the internal built-in field at the p-n junction and reduces the depletion layer width and therefore increases the n-type channel width. In low-temperature operation below T_C , the increase of the critical supercurrent in the Josephson junction property was observed with a gate forward bias up to 0.8 V.²⁷⁾ This demonstrates that electron Cooper pairs are flowing in the area very close to the depletion layer at the p-n junction and that an enhanced forward bias leads to the injection of electron Cooper pairs into the CP-LED active layer.

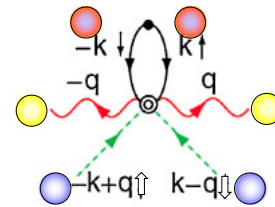


Fig. 4. (Color online) Schematic illustration of the dominant recombination process where an electron Cooper-pair recombines with a pair of holes.

3. Theoretical Treatment of Cooper-Pair Radiative Recombination

For the discussion of the relation of IQE and radiative lifetimes measured on CP-LEDs, the main points of the theoretical analysis of Cooper-pair radiative recombination²⁶⁾ are given as follows. In a p-type Sm-S junction under local equilibrium, radiative recombination between an electron Cooper pair and a pair of holes is considered. The expectation number of photons is calculated based on the second-order perturbation theory including a perturbation Hamiltonian due to the corresponding optical dipole transition. The superconductivity was included with the Bogoliubov transformation, which is the conversion from normal creation and annihilation operators into Bogoliubov quasiparticle creation and annihilation operators.³⁷⁾ Among twelve terms derived from the theoretical treatment, the most dominant term is schematically illustrated in Fig. 4. An electron with momentum k and spin \uparrow forms a spin singlet state with an electron with momentum $-k$ and spin \downarrow . They recombine with a pair of holes with momentum $k-q$ and spin \downarrow and momentum $-k+q$ and spin \uparrow . This generates an indistinguishable pair of photons with momentum of q and $-q$. The spin-singlet pair of electrons corresponds to the formation of an electron Cooper pair and the complete process describes the recombination of an electron Cooper pair with a pair of holes. This term shows singular behavior under momentum and energy conservation and is evaluated by introducing a finite relaxation time.²⁶⁾

Figure 5 displays the luminescence intensity calculated with the relaxation time τ due to elastic impurity scattering (inelastic scattering is also considered in ref. 26). Δ_0 is half the superconducting energy gap (pair potential) at zero temperature. The enhancement of the luminescence intensity for lowering the temperature below T_C is clearly shown in Fig. 5, and the radiative recombination rate is analytically expressed in the following form:²⁶⁾

$$\begin{aligned}
 W &= \frac{1}{\tau_{\text{rad,super}}} \\
 &\approx |M|^4 N_0 \frac{\Delta^2(T)}{T} \exp\left[-\frac{2L_W}{\xi_N(T)}\right] \sum_{q,\sigma} \frac{\tau}{\Gamma} \\
 &\equiv A \frac{\Delta^2(T)}{T} \exp\left[-\frac{2L_W}{\xi_N(T)}\right], \quad (1)
 \end{aligned}$$

where $\tau_{\text{rad,super}}$ is the minority carrier (hole) lifetime due to their radiative recombination with electron Cooper pairs in the active layer, M is the optical dipole transition amplitude,

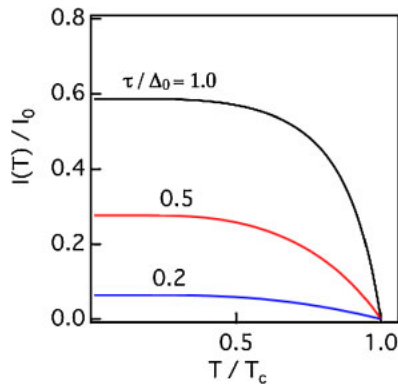


Fig. 5. (Color online) Theoretically calculated normalized luminescence intensity versus temperature below the superconducting critical temperature T_c .

N_0 is the normal density of states in a superconductor at the Fermi energy, $\Delta(T)$ is the temperature dependent half of the superconducting energy gap, τ is a relaxation time (either elastic or inelastic) related to the optical transitions, and Γ is a more generalized relaxation term including the transfer process of Cooper pairs from the barrier layer to the active layer. The term of $\exp[-2L_W/\xi_N(T)]$ is phenomenologically introduced to take the proximity effect into account; L_W is the distance from the S–Sm interface to the active layer and ξ_N is the coherence length of Cooper pairs in the normal medium (InGaAs semiconductor). This term is also derived with a Green function formalism (refs. 38 and 39). In the present CP-LEDs, L_W is ~ 40 nm, which is much shorter than ξ_N in the main part of the temperature range.^{27,30} Among the several terms in eq. (1), the temperature dependence is dominated by $\Delta(T)$ near T_c ⁴⁰ and by $1/T$ for the lower temperature range. The other parameters were merged to one single fitting parameter A in ref. 30.

4. Transient Lifetime Measurements of CP-LED

One of the key methods to discuss the optical properties of a device, such as optical efficiencies or recombination rates, is the measurement of their radiative lifetime. One possible approach is to measure the luminescence transient decay after pulsed photo-excitation. This is the method employed in ref. 30. A more direct correlation with LED operations is possible with electrical measurements. However, this is experimentally more challenging because the circuit capacitance–resistance (CR) time delay has to be taken into

account. The method to derive the intrinsic luminescence decay from the electrical measurements was briefly discussed in ref. 27; more details will be discussed later in this section.

Our LED in the cryostat is connected with an external pulse generator and DC bias circuits via a coaxial cable and electric wires. These connected circuits result in a CR time delay of the pulsed current injected into the LED. The photon generation process in the n-type InGaAs active layer is limited by the minority carrier (hole) injection, and the dynamics of the hole injection is given by the following rate equation:

$$\frac{dp(t)}{dt} = G(t) - \frac{p(t)}{\tau_{\text{LED}}}, \quad (2)$$

where $p(t)$ is the time-dependent hole concentration and the current term is given by

$$G(t) = \begin{cases} J_0 & \text{for } t \leq 0 \\ J_0 \exp\left(-\frac{t}{\tau_{\text{CR}}}\right) & \text{for } t \geq 0 \end{cases} \quad (3)$$

J_0 is the steady-state carrier injection rate, which is the injection current divided by the electron charge and τ_{LED} is the hole recombination lifetime in the LED. For the transient measurements, the constant carrier injection rate J_0 for $t \leq 0$ is turned off at $t = 0$, but the circuit CR time delay gives the transient exponential decay. During the steady state for $t \leq 0$ the carrier injection rate becomes

$$J_0 = \frac{p_0}{\tau_{\text{LED}}}, \quad (4)$$

and therefore the steady-state hole concentration is given by

$$p_0 = J_0 \tau_{\text{LED}}. \quad (5)$$

For $t \geq 0$, the solution of the differential eq. (2) is given by

$$p(t) = a \exp\left(-\frac{t}{\tau_{\text{LED}}}\right) + \frac{J_0}{\tau_{\text{LED}}^{-1} - \tau_{\text{CR}}^{-1}} \exp\left(-\frac{t}{\tau_{\text{CR}}}\right). \quad (6)$$

Considering the initial condition at $t = 0$, the constant a is determined as

$$a = J_0 \tau_{\text{LED}} - \frac{J_0}{\tau_{\text{LED}}^{-1} - \tau_{\text{CR}}^{-1}}. \quad (7)$$

Consequently, the LED output (output photon number, which is the EL integrated intensity divided by the photon energy) is given by

$$\begin{aligned} I_{\text{EL}}(t) &= \eta_{\text{int}} \eta_{\text{det}} \frac{p(t)}{\tau_{\text{LED}}} \\ &= J_0 \eta_{\text{int}} \eta_{\text{det}} \left\{ \left(1 - \frac{1}{1 - \frac{\tau_{\text{LED}}}{\tau_{\text{CR}}}} \right) \exp\left(-\frac{t}{\tau_{\text{LED}}}\right) + \frac{1}{1 - \frac{\tau_{\text{LED}}}{\tau_{\text{CR}}}} \exp\left(-\frac{t}{\tau_{\text{CR}}}\right) \right\} \\ &= J_0 \eta_{\text{int}} \eta_{\text{det}} \left\{ \exp\left(-\frac{t}{\tau_{\text{LED}}}\right) + \frac{1}{1 - \frac{\tau_{\text{LED}}}{\tau_{\text{CR}}}} \left[-\exp\left(-\frac{t}{\tau_{\text{LED}}}\right) + \exp\left(-\frac{t}{\tau_{\text{CR}}}\right) \right] \right\}, \quad (8) \end{aligned}$$

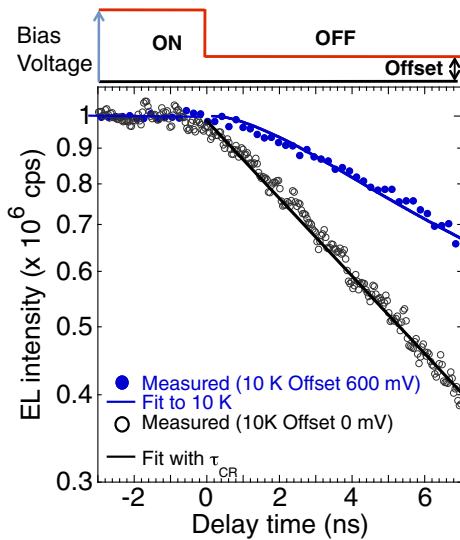


Fig. 6. (Color online) CP-LED transient EL decay measured at different offset bias. The decay with 0 mV offset is single exponential, as given by eq. (9), and temperature independent (no variation between 3 and 10 K within measurement errors). The decay with 600 mV offset follows eq. (8) and is temperature dependent.

where η_{int} and η_{det} are the LED IQE and the external photon detection efficiency, respectively. For the purpose of estimating the LED decay time τ_{LED} , it is important to find an appropriate way how to determine the circuit CR constant τ_{CR} . If we assume the case where the LED has an extremely fast decay so that $\tau_{\text{LED}} \ll \tau_{\text{CR}}$, eq. (8) can be simplified to

$$I_{\text{EL}}(t) = J_0 \eta_{\text{int}} \eta_{\text{det}} \exp\left(-\frac{t}{\tau_{\text{CR}}}\right). \quad (9)$$

In this case the transient response is not limited by the LED but by the circuit CR delay time. This situation has been reported in ref. 41, where the flat-band condition under forward bias is changed with step-wise voltage drop and electrons and holes in the active layer suddenly become exposed to the internal built-in field. This internal field induces the Stark effect and the electrons and holes are swiftly separated in space. In the case of ref. 41, the LED decay of 2.14 ns under forward bias is reduced to 0.18 ns with this Stark effect. The latter decay time of 0.18 ns is limited by the CR time constant of the system.

The above discussion on the LED decay time originates from the fact that LED responses are generally limited by the dynamics of injected minority carriers. This situation is the same in the present CP-LED regardless of whether the Nb electrodes are in the superconductive state or not. CP-LED EL output was observed from the slit opening shown in Fig. 2. The black open circles in Fig. 6 were measured with zero offset voltage for $t \geq 0$ and the solid line is the fit with eq. (9) for the time range of $t \geq 0$. The CR time constant was measured to be 2.70 ns and was much longer than the 0.18 ns in ref. 41. This is because the experimental setup of ref. 41 is open to air and can minimize the electrical wiring to the LED. In our case the CP-LED is mounted in a cryostat to enable cooling to 0.3 K for measuring the superconducting properties. This requires significantly longer wiring to prevent heat transfer to the CP-LED as well as additional

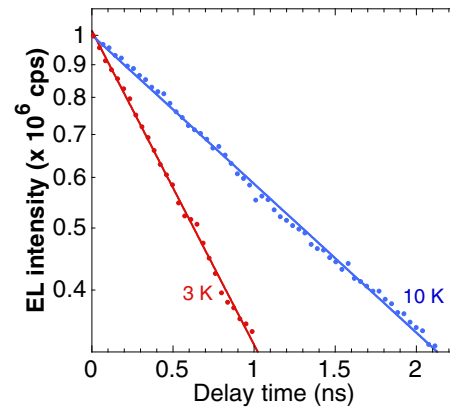


Fig. 7. (Color online) Temperature dependence of intrinsic transient CP-LED decay at 3 and 10 K.

connectors and therefore results in the longer CR time constant. This CR time constant originates from electrical connections to the external pulse generator and DC bias circuits with most of them not much cooled. Therefore the temperature dependence of the CR time constant was negligible within our measurement errors below and above T_C (not shown but experimentally confirmed).

Since τ_{CR} is evaluated and fixed as demonstrated above, the LED decay time τ_{LED} is determined by the fit to the measurement data using eq. (8). The offset bias was determined such that the p-n junction is almost in flat-band condition with only a minimal forward current remaining; then it was changed to the diode forward bias of 600 mV. The blue solid line is the fit to the measurement data at 10 K shown by the closed circles with τ_{LED} of 2.27 ns. From these kinds of fits it is possible to reproduce the intrinsic time response of the LED from each data set by employing eq. (8); the results are shown in Fig. 7. The Nb superconducting T_C is 7.3 K in this device and the CP-LED decay at 3 and 10 K shows substantial difference below and above T_C .

5. Relation of IQE and Radiative Lifetime

In this section the relation of the temperature dependence of CP-LED EL decay and integrated EL intensity, which is proportional to IQE, is discussed in detail.

5.1 General formula for IQE and radiative lifetime

The steady-state EL integrated intensity measured from the CP-LED divided by the photon energy is the output photon number and is given by

$$I_{\text{EL}} = J_0 \eta_{\text{int}} \eta_{\text{det}}, \quad (10)$$

where the definition of J_0 , η_{int} , and η_{det} are the same as those in eq. (8). The IQE of the CP-LED is given by

$$\eta_{\text{int}} = \frac{\tau_{\text{rad}}^{-1}}{\tau_{\text{rad}}^{-1} + \tau_{\text{nonrad}}^{-1}}, \quad (11)$$

where τ_{rad} and τ_{nonrad} are the radiative and nonradiative lifetimes, respectively. The relation to the measured CP-LED decay time τ_{LED} is given by

$$\tau_{\text{LED}}^{-1} = \tau_{\text{rad}}^{-1} + \tau_{\text{nonrad}}^{-1}, \quad (12)$$

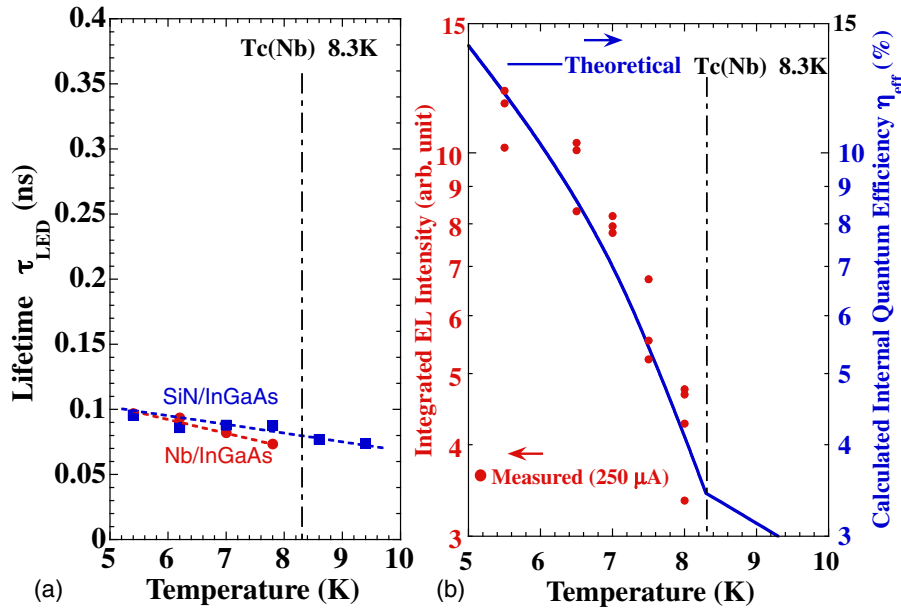


Fig. 8. (Color online) Temperature dependence of (a) luminescence lifetime measured with ps-pulsed laser excitation on the Nb-slit surface (Nb/InGaAs) and on the SiN-covered surface (SiN/InGaAs) of a CP-LED with low IQE (with the respective excitation power of 160 and 80 μ W) and (b) EL intensity measured on the CP-LED with the constant injection current of 250 μ A. The solid line is the theoretical fit to the measurements.

In the present case, τ_{rad} has two contributions, one from normal electron recombination and the other from electron Cooper-pair recombination, i.e.,

$$\tau_{\text{rad}}^{-1} = \tau_{\text{rad,normal}}^{-1} + \tau_{\text{rad,super}}^{-1}, \quad (13)$$

where $\tau_{\text{rad,super}}$ is given by eq. (1) and is highly temperature dependent below T_C .

5.2 CP-LED with low internal quantum efficiency

In 2008, we observed drastic enhancement of integrated EL intensity from a CP-LED at temperatures below Nb T_C .²⁵ The measurement of the CP-LED decay time was not possible with this device due to the lower total EL output. Therefore, the luminescence decay was measured with ps-pulsed photoexcitation.³⁰ The major results are summarized in Fig. 8(a). Under the constant injection current of 250 μ A, drastic enhancement of the EL output was observed below T_C of 8.3 K as shown in Fig. 8(b). However the observed lifetime was on the order of 100 ps and the temperature dependence was moderate above and below T_C . The lifetime measured on the Nb-slit surface (designated as Nb/InGaAs) was on the same order as the one measured on the same CP-LED device surface passivated with the SiN layer shown in Fig. 2 (designated as SiN/InGaAs).

Following the formalism given in §5.1, the observed short lifetime suggests

$$\begin{aligned} \tau_{\text{LED}}^{-1} &= \tau_{\text{rad}}^{-1} + \tau_{\text{nonrad}}^{-1} \\ &\approx \tau_{\text{nonrad}}^{-1} \text{ or } \tau_{\text{rad}} \gg \tau_{\text{nonrad}}. \end{aligned} \quad (14)$$

Then the IQE is given by

$$\begin{aligned} \eta_{\text{int}} &= \frac{\tau_{\text{rad}}^{-1}}{\tau_{\text{rad}}^{-1} + \tau_{\text{nonrad}}^{-1}} \\ &\approx \frac{\tau_{\text{rad,normal}}^{-1} + \tau_{\text{rad,super}}(T)^{-1}}{\tau_{\text{nonrad}}^{-1}}. \end{aligned} \quad (15)$$

The temperature dependence (T) was added to the term $\tau_{\text{rad,super}}$ to highlight the temperature dependence introduced in eq. (1). Since the temperature dependence of this term dominates the other terms, the increase of IQE is directly transferred to the increase of the integrated EL intensity that is given by

$$\begin{aligned} I_{\text{EL}} &= J_0 \eta_{\text{int}} \eta_{\text{det}} \\ &\approx J_0 \eta_{\text{det}} \tau_{\text{nonrad}} [\tau_{\text{rad,normal}}^{-1} + \tau_{\text{rad,super}}(T)^{-1}], \end{aligned} \quad (16)$$

where the second term in the parentheses dominates below T_C . The total CP-LED lifetime is dominated by τ_{nonrad} as shown in eq. (14) and is thus almost insensitive to a temperature change across T_C as shown in Fig. 8(a).

The IQE of this CP-LED can be evaluated by quantitative measurements of the integrated EL outputs and lifetimes of the CP-LED based on the relations of eqs. (1) and (10)–(13).³⁰ The solid line in Fig. 8(b) is the theoretical fit to the measured integrated EL intensity and IQE was estimated to be less than 12% in the measured temperature range.

5.3 CP-LED with high internal quantum efficiency ($\sim 100\%$)

The optical quality of the CP-LEDs could be successfully improved in 2009 and much higher EL output was obtained. This made the electrical pulsed lifetime measurements discussed in §4 possible. The CP-LED EL decay times τ_{LED} (hole lifetimes) measured above T_C were ~ 2.25 ns and were almost the same as those measured on a reference LED without Nb electrodes as shown in Fig. 9(a). Concerning InGaAs layers lattice matched to InP there have been active studies of related lifetimes. The B coefficient for a series of p- and n-type doped InGaAs has been determined to be $1.43 \times 10^{-10} \text{ cm}^{-3} \text{ s}^{-1}$, with the normal radiative lifetime given by $\tau_{\text{rad,normal}} = 1/(BN)$.⁴² The majority-carrier (electron) concentration N in n-InGaAs layers with $\tau_{\text{rad,normal}} \sim 2.25$ ns is $3.1 \times 10^{18} \text{ cm}^{-3} \text{ s}^{-1}$

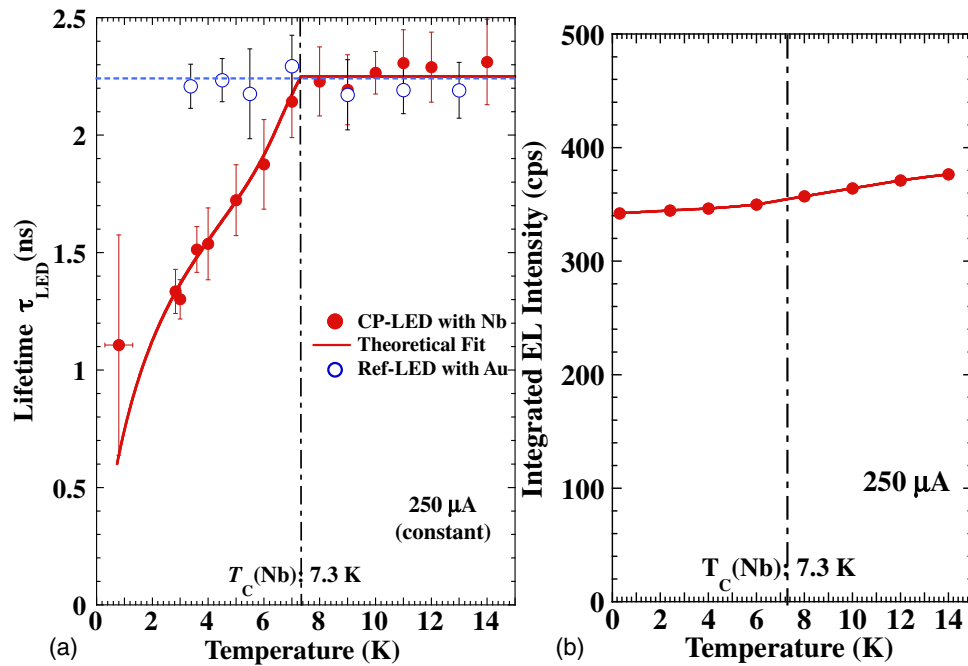


Fig. 9. (Color online) Temperature dependence of (a) luminescence lifetime and (b) EL intensity measured on a CP-LED with high IQE. Open circles in (a) are measurements on a reference LED with the superconducting Nb electrodes replaced by normal conducting Au electrodes.

which is in a reasonable range considering the doping level of the respective layers of the CP-LED samples.^{25,27)} The measured CP-LED lifetime now shows an abrupt decrease below T_C . Equations (12) and (13) are rearranged as

$$\tau_{\text{LED}}^{-1} = (\tau_{\text{rad,normal}}^{-1} + \tau_{\text{nonrad}}^{-1}) + \tau_{\text{rad,super}}(T)^{-1}, \quad (17)$$

where the terms in parenthesis correspond to the reference LED and the abrupt decrease of the lifetime below T_C is the contribution of $\tau_{\text{rad,super}}(T)$. The solid line is the theoretical fit to the measured lifetime using eq. (17) together with eq. (1). The huge error bar shown for the value at 0.8 K is due to our continuous flow He-3 cryostat. In the temperature range down to 3 K, the CP-LED was cooled with a conventional pulse-tube refrigerator. Below 3 K our cryostat employs a liquid He-3 pot which cools the sample down to 0.3 K with the heat of vaporization of the liquid He-3. However this cooling power is limited. Also we are injecting current into the CP-LED and heating of the device is not negligible especially due to the 50-Ohm terminations used for the high-speed pulse current injection. This limited our measurement time and the accuracy of the measured τ_{LED} values at 0.8 K.

In spite of the abrupt change of lifetime below T_C , the CP-LED EL output was almost insensitive below and above T_C as shown in Fig. 9(b). The IQE in this case is

$$\begin{aligned} \eta_{\text{int}} &= \frac{\tau_{\text{rad}}^{-1}}{\tau_{\text{rad}}^{-1} + \tau_{\text{nonrad}}^{-1}} \\ &\approx \frac{\tau_{\text{rad,normal}}^{-1} + \tau_{\text{rad,super}}(T)^{-1}}{\tau_{\text{rad,normal}}^{-1} + \tau_{\text{rad,super}}(T)^{-1}} \\ &= 1. \end{aligned} \quad (18)$$

Thus the EL output under constant injection current is given by

$$I_{\text{EL}} = J_0 \eta_{\text{int}} \eta_{\text{det}} \approx J_0 \eta_{\text{det}}, \quad (19)$$

and the EL output does not depend on the change of $\tau_{\text{rad,super}}(T)$. This explains the nearly constant EL output across T_C . The equivalent relation of $\tau_{\text{rad}} \ll \tau_{\text{nonrad}}$ is rationalized by the above discussion based on the known B coefficient and therefore becomes

$$\begin{aligned} \tau_{\text{LED}}^{-1} &= \tau_{\text{rad}}^{-1} + \tau_{\text{nonrad}}^{-1} \approx \tau_{\text{rad}}^{-1} \\ &= \tau_{\text{rad,normal}}^{-1} + \tau_{\text{rad,super}}(T)^{-1}. \end{aligned} \quad (20)$$

We want to discuss the slight increase of the EL output with temperature in Fig. 9(b), where the EL output increases about 10% at 14 K relative to that at 0.3 K. If this is due to a remaining contribution of the τ_{nonrad} term in eq. (18), the difference of the numerator and denominator in eq. (18) becomes larger for higher temperatures, and consequently, the EL output (or IQE) decreases. This trend is opposite to the observation of the temperature dependence of the higher IQE shown in Fig. 9(b). In the present CP-LEDs without tight quantum confinement, the recombination area is defined by the minority hole injection and hole diffusion in the n-InGaAs layer. This spatial diffusion of injected holes modifies the present EL output from the Nb slit opening with a width of ~ 100 nm and also induces the residual temperature dependence.

6. Transient Photon Emission from CP-LED

During the pulsed measurements of CP-LEDs, many parameters such as the diode bias, the built-in field across the p-n junction, the depletion layer width at the p-n junction, electron Cooper-pair injection, and hole injection are transiently modified, and the situation is conceptually not simple. Especially in view of Fig. 7, the integrated EL intensity (photon number) emitted during the transient decay is reduced at 3 K (about half of that at 10 K).

The EL decay for $t \geq 0$ shown in Fig. 7 is given by

$$I_{\text{EL}}(t) = I_{\text{EL}}(t=0) \exp\left(-\frac{t}{\tau_{\text{LED}}}\right) t \geq 0. \quad (21)$$

The total photon number emitted during the transient decay is given by the integration of eq. (21), which is,

$$N_{\text{photon}} = \int_0^{\infty} I_{\text{EL}}(t) dt = I_{\text{EL}}(t=0) \tau_{\text{LED}}. \quad (22)$$

This equation shows that the total photon number N_{photon} emitted during the transient decay is proportional to the CP-LED lifetime because the steady state EL output $I_{\text{EL}}(t=0)$ is constant regardless of the variation of τ_{LED} , as discussed with eqs. (18) and (19). Therefore N_{photon} naturally decreases when τ_{LED} decreases, as can be seen in Fig. 7.

Following the discussion in §5.3, $\tau_{\text{LED}}(T) \approx \tau_{\text{rad}}(T)$ and the steady-state minority hole concentration is related to the carrier injection rate J_0 with eq. (4), which is,

$$J_0 = \frac{p_0}{\tau_{\text{LED}}} \approx \frac{p_0(T)}{\tau_{\text{rad}}(T)}. \quad (23)$$

Under constant J_0 , the EL output remains constant, too. When the lifetime $\tau_{\text{rad}}(T)$ decreases below T_C , $p_0(T)$ also decreases in accordance with eq. (23), which leads to

$$p_0(3 \text{ K}) = p_0(10 \text{ K}) \frac{\tau_{\text{LED}}(3 \text{ K})}{\tau_{\text{LED}}(10 \text{ K})}. \quad (24)$$

This equation shows that the steady-state hole concentration at 3 K is reduced with the reduction of the CP-LED lifetime. This results in the reduction of the emitted photon number during the transient decay at 3 K. This simple rate equation analysis shows the self-consistency of our observations.

7. Electron Cooper-Pair Recombination vs Normal Electron Recombination

Concerning the case discussed in §5.3, the contribution of electron Cooper pairs and normal electrons to the EL output is quantitatively discussed. Reorganizing eqs. (10) and (11) as well as considering the condition given by eq. (18), the EL intensity can be given as

$$\begin{aligned} I_{\text{EL}} &\approx J_0 \eta_{\text{det}} \tau_{\text{LED}} [\tau_{\text{rad,normal}}^{-1} + \tau_{\text{rad,super}}(T)^{-1}] \\ &\equiv I_{\text{EL,Normal}} + I_{\text{EL,Cooper-pair}}. \end{aligned} \quad (25)$$

Therefore the ratio of normal-electron and Cooper-pair contributions can be directly determined by the respective radiative lifetimes. According to the data displayed in Fig. 9 the radiative lifetime related to normal electrons $\tau_{\text{rad,normal}}$ is ~ 2.25 ns. This value could be obtained from both the data of the reference LED and the data of CP-LED above T_C , and it is, furthermore, temperature independent within the measurement errors. Therefore it can be fixed to 2.25 ns. The Cooper-pair radiative lifetime $\tau_{\text{rad,super}}$ is calculated from the measured CP-LED lifetime τ_{LED} employing eq. (20). The contributions of electron Cooper-pairs and normal electrons to the radiative recombination are determined from these lifetime data and are shown in Fig. 10. The solid lines are calculated from the theoretical fit (solid line) in Fig. 9(a). The Cooper-pair contribution dramatically increases below T_C and is at least comparable to the normal electron contribution at 2 K in this CP-LED.

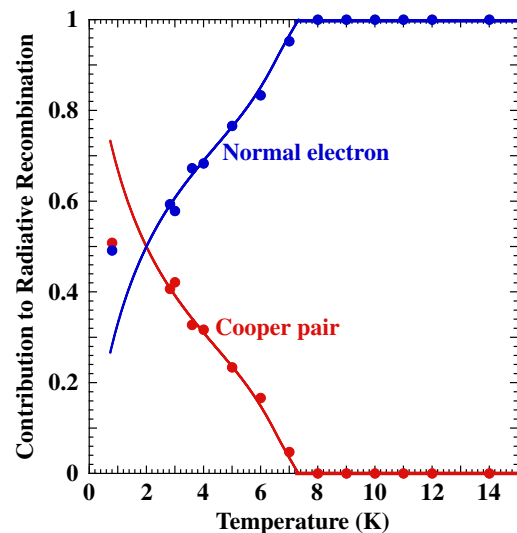


Fig. 10. (Color online) Temperature dependence of the contribution of electron Cooper-pair recombination and normal electron recombination to the total interband radiative recombination in a CP-LED. The solid lines are theoretical calculations based on Fig. 9.

8. Conclusions

The relation of IQE and radiative lifetime in a CP-LED was formulated and the mutual relation was clarified. The drastic enhancement of EL output observed below T_C was due to the higher Cooper-pair-based radiative recombination rate, but this observation was only possible when the IQE was low and the CP-LED lifetime was dominated by nonradiative recombination. For CP-LEDs with higher IQE, the reduction of radiative lifetime due to the Cooper-pair recombination was directly observable, but the EL output remained constant due to the high IQE close to 100%. These apparently quite different LED performances were clearly explained with the presented formulation. The contribution of the Cooper-pair recombination to the EL output was quantitatively evaluated and found to be at least equivalent to that of normal electrons in the case of low temperature.

Before our research the interaction of high-energy photons (photon energy ~ 1 eV) with Cooper pairs was limited to destructive absorption processes.⁴³ The main difference in CP-LED is that Cooper-pairs are the initial state for radiative recombination with holes and coherent dipole interactions are possible. The successful operation of CP-LEDs represents an essential step toward developing an interdisciplinary field connecting superconductivity and optoelectronics as well as quantum optics. Recently, a more phase-sensitive Josephson LED was theoretically proposed.⁴⁴ Our Josephson junction measurements on CP-LEDs showed some correlations of the critical supercurrent and photon generation inside the CP-LED.²⁹ More detailed experimental studies will clarify this phase sensitivity in the near future.

Acknowledgments

The authors are grateful to Dr. Hirofumi Kan and Dr. Masamichi Yamanishi of Hamamatsu Photonics for their encouragement and fruitful discussions. C.H. acknowledges the Japan Society for the Promotion of Science (JSPS) for providing financial support in the form of a JSPS Fellowship for Foreign Researchers.

- 1) J. H. Plantenberg, P. C. de Groot, C. J. P. M. Harmans, and J. E. Mooij: *Nature* **447** (2007) 836.
- 2) R. McDermott, R. W. Simmonds, M. Steffen, K. B. Cooper, K. Cicak, K. Osborn, S. Oh, D. P. Pappas, and J. M. Martinis: *Science* **307** (2005) 1299.
- 3) S. Saito, M. Thorwart, H. Tanaka, M. Ueda, H. Nakano, K. Semba, and H. Takayanagi: *Phys. Rev. Lett.* **93** (2004) 37001.
- 4) A. O. Niskanen, K. Harrabi, F. Yoshihara, Y. Nakamura, S. Lloyd, and J. S. Tsai: *Science* **316** (2007) 723.
- 5) R. Ursin, F. Tiefenbacher, T. Schmitt-Manderbach, H. Weier, T. Scheidl, M. Lindenthal, B. Blauensteiner, T. Jennewein, J. Perdigues, P. Trojek, B. Oemer, M. Fürst, M. Meyenburg, J. Rarity, Z. Sodnik, C. Barbieri, H. Weinfurter, and A. Zeilinger: *Nat. Phys.* **3** (2007) 481.
- 6) SECOQC Quantum Backbone (QBB)-links (fiber ring network) (October 2008) [http://www.secoqc.net/html/conference/].
- 7) Tokyo QKD (Quantum Key Distribution) Network Operation during October 18–20, 2010 UQCC (Updating Quantum Cryptography and Communications) [http://www.uqcc2010.org/highlights/index.html].
- 8) K. Takemoto, Y. Nambu, T. Miyazawa, K. Wakui, S. Hirose, T. Usuki, M. Takatsu, N. Yokoyama, K. Yoshino, A. Tomita, S. Yorozu, Y. Sakuma, and Y. Arakawa: *Appl. Phys. Express* **3** (2010) 092802.
- 9) C. H. Bennett, G. Brassard, and N. D. Mermin: *Phys. Rev. Lett.* **68** (1992) 557.
- 10) A. Zeilinger, M. A. Horne, H. Weinfurter, and M. Zukowski: *Phys. Rev. Lett.* **78** (1997) 3031.
- 11) C. H. Bennett, G. Brassard, and N. D. Mermin: *Phys. Rev. Lett.* **68** (1992) 557.
- 12) C. H. Bennett, G. Brassard, C. Crépeau, R. Jozsa, A. Peres, and W. K. Wootters: *Phys. Rev. Lett.* **70** (1993) 1895.
- 13) D. Bouwmeester, J. W. Pan, K. Mattle, H. Weinfurter, and A. Zeilinger: *Nature* **390** (1997) 575.
- 14) P. G. Kwiat, K. Mattle, H. Weinfurter, A. Zeilinger, A. V. Sergienko, and Y. Shih: *Phys. Rev. Lett.* **75** (1995) 4337.
- 15) N. V. Korol'kova and A. S. Chirkin: *Quantum Electron.* **28** (1998) 285.
- 16) R. M. Stevenson, R. J. Young, P. Atkinson, K. Cooper, D. A. Ritchie, and A. J. Shields: *Nature* **439** (2006) 179.
- 17) A. Dousse, J. Suffczynski, A. Beveratos, O. Krebs, A. Lemaitre, I. Sagnes, J. Bloch, P. Voisin, and P. Senellart: *Nature* **466** (2010) 217.
- 18) A. Mohan, M. Felici, P. Gallo, B. Dwir, A. Rudra, J. Faist, and E. Kapon: *Nat. Photonics* **4** (2010) 302.
- 19) C. L. Salter, R. M. Stevenson, I. Farrer, C. A. Nicoll, D. A. Ritchie, and A. J. Shields: *Nature* **465** (2010) 594.
- 20) K. Edamatsu, G. Oohata, R. Shimizu, and T. Itoh: *Nature* **431** (2004) 167.
- 21) K. Edamatsu: *Jpn. J. Appl. Phys.* **46** (2007) 7175.
- 22) A. Hayat, P. Ginzburg, and M. Orenstein: *Nat. Photonics* **2** (2008) 238.
- 23) E. Hanamura: *Phys. Status Solidi B* **234** (2002) 166.
- 24) I. Suemune, T. Akazaki, K. Tanaka, M. Jo, K. Uesugi, M. Endo, H. Kumano, E. Hanamura, H. Takayanagi, M. Yamanishi, and H. Kan: *Jpn. J. Appl. Phys.* **45** (2006) 9264.
- 25) Y. Hayashi, K. Tanaka, T. Akazaki, M. Jo, H. Kumano, and I. Suemune: *Appl. Phys. Express* **1** (2008) 011701.
- 26) Y. Asano, I. Suemune, H. Takayanagi, and E. Hanamura: *Phys. Rev. Lett.* **103** (2009) 187001.
- 27) H. Sasakura, S. Kuramitsu, Y. Hayashi, K. Tanaka, T. Akazaki, E. Hanamura, R. Inoue, H. Takayanagi, Y. Asano, C. Hermannstädter, H. Kumano, and I. Suemune: *Phys. Rev. Lett.* **107** (2011) 157403.
- 28) P. G. de Gennes: *Superconductivity of Metals and Alloys* (Westview Press, ABP, CO, 1999).
- 29) R. Inoue, H. Takayanagi, T. Akazaki, K. Tanaka, and I. Suemune: *Supercond. Sci. Technol.* **23** (2010) 034025.
- 30) I. Suemune, Y. Hayashi, S. Kuramitsu, K. Tanaka, T. Akazaki, H. Sasakura, R. Inoue, H. Takayanagi, Y. Asano, E. Hanamura, S. Odashima, and H. Kumano: *Appl. Phys. Express* **3** (2010) 054001.
- 31) J.-H. Huh, C. Hermannstädter, H. Sato, S. Ito, Y. Idutsu, H. Sasakura, K. Tanaka, T. Akazaki, and I. Suemune: *Nanotechnology* **22** (2011) 045302.
- 32) H. Takayanagi, R. Inoue, T. Akazaki, K. Tanaka, and I. Suemune: *Physica C* **470** (2010) 814.
- 33) G. E. Blonder, M. Tinkham, and T. M. Klapwijk: *Phys. Rev. B* **25** (1982) 4515.
- 34) K. Kajiyama, Y. Mizushima, and S. Sakata: *Appl. Phys. Lett.* **23** (1973) 458.
- 35) I. Suemune, T. Akazaki, K. Tanaka, M. Jo, K. Uesugi, M. Endo, H. Kumano, and E. Hanamura: *Microelectron. J.* **39** (2008) 344.
- 36) Y. Hayashi, K. Tanaka, T. Akazaki, M. Jo, H. Kumano, and I. Suemune: *Phys. Status Solidi C* **5** (2008) 2816.
- 37) J. Unterhinninghofen, D. Manske, and A. Knorr: *Phys. Rev. B* **77** (2008) 180509(R).
- 38) R. D. Parks: *Superconductivity* (Marcel Dekker, New York, 1969).
- 39) J. B. Ketterson and S. N. Song: *Superconductivity* (Cambridge University Press, Cambridge, U.K., 1999).
- 40) J. R. Schrieffer: *Theory of Superconductivity* (Westview Press, Oxford, U.K., 1999) p. 44.
- 41) A. J. Bennett, D. C. Unitt, P. See, A. J. Shields, P. Atkinson, K. Cooper, and D. A. Ritchie: *Phys. Rev. B* **72** (2005) 033316.
- 42) R. K. Ahrenkiel, R. Ellingson, S. Johnston, and M. Wanlass: *Appl. Phys. Lett.* **72** (1998) 3470.
- 43) R. Sobolewski, A. Verevkin, G. N. Goltsman, A. Lipatov, and K. Wilsher: *IEEE Trans. Appl. Supercond.* **13** (2003) 1151.
- 44) R. Recher, Y. V. Nazarov, and L. P. Kouwenhoven: *Phys. Rev. Lett.* **104** (2010) 156802.



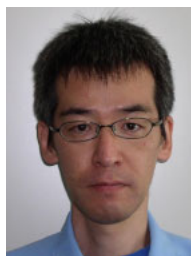
Ikuo Suemune received his Doctor degree in Physical Electronics from the Tokyo Institute of Technology in 1977. In April 1993, he joined the Research Institute for Electronic Science (RIES) of the Hokkaido University, Japan, where he is a Professor. He leads the Nano-photonics Laboratory in the Nanotechnology Research Center of the RIES in the Hokkaido University. His major interest includes single dot spectroscopy and “Superconducting photonics”. He has authored or coauthored more than 300 refereed journal publications, nearly 50 invited talks in international conferences, and more than 15 invited book chapters. He is a member of the Japan Society of Applied Physics and American Physical Society.



Hirotaka Sasakura received the Ph. D. degree from Hokkaido University, Japan, in 2003. From 2002 to 2003, he was a researcher supported by research fellowships for young scientists from JSPS. He is currently a research associate in the Research Institute for Electronic Science (RIES), Hokkaido University. His research interests include magneto-optical properties of exciton- and nuclear-spin in semiconductor nanoscale structure. He received the 24th JSAP young scientist award for the presentation of an excellent paper in 2008.



Yujiro Hayashi received his Ph. D. degree in X-ray Engineering from Kyushu University, Japan, in 2006. He joined Research Institute for Electronic Science of Hokkaido University, Japan, as a postdoctoral research associate in 2006. He received a postdoctoral fellowship from the Japan Society for the Promotion of Science in 2007. He has worked as a researcher in Toyota Central R&D Labs., Inc., Japan, since 2008 and has developed analysis methods using synchrotron radiation for automotive materials.



Kazunori Tanaka was born in Hiroshima, Japan, in 1969. He received the B.S. and M.S. degrees in engineering from Hiroshima University, Hiroshima, Japan, in 1992 and 1994, respectively. He joined Hamamatsu Photonics K.K., Shizuoka, Japan, in April 1994. His current research interests include semiconductor lasers, light emitting diodes, and metamaterials. Mr. Tanaka is a member of the Japan Society of Applied Physics.



Tatsushi Akazaki received the B.S. and M.S. degrees in Physics from Kyushu University, Fukuoka, Japan, in 1984 and 1986, respectively. He joined NTT Basic Research Laboratories, Japan, in 1986, where he received the Ph. D. degree in Engineering of electricity from Osaka University in 1995. Since 1986, he has been engaged in research on the transport properties of the semiconductor-coupled superconducting devices. He is a member of the Physical Society of Japan and the Japan

Society of Applied Physics.



Yasuhiro Asano received the D. Eng. in Applied Physics from the Graduate School of Engineering, Nagoya University in 1995. He has been engaged in theory of solid state physics and has done important contribution in theory of superconducting hybrid structures.



Ryotaro Inoue received B.S., M.S. and Ph. D. degree from University of Tokyo, Tokyo, Japan, in 1998, 2000, and 2003, respectively. From 2003 to 2004, he was a postdoctoral researcher and engaged in the development of measurement system of microwave and terahertz wave. Since April 2007, he has been an Assistant Professor in Takayanagi Laboratory, Tokyo University of Science. His current research interests are the developments of measurement technique from microwave to terahertz frequency region, and its application to the quantum measurement. He is a member of the Japan Society of Applied Physics and the Physical Society of Japan.

He is a member of the Japan Society of Applied Physics and the Physical Society of Japan.



Hideaki Takayanagi after he received a master degree from the University of Tokyo in 1977, he joined NTT Basic Research Laboratory. He studied physics of superconducting devices there for a long time. He became a director of NTT Basic Research Laboratories in 2003 and joined Tokyo University of Science in 2005. He is now a governor and a professor of Research Institute for Science and Technology. He is a specialist of mesoscopic superconductivity.



Eiichi Hanamura received the BSc and doctor degree in Engineering from the University of Tokyo in 1960 and 1965, respectively. He joined the University of Tokyo as a Research Associate in 1965, an Associated Professor in 1966, and a Professor in 1974. In 1998 he joined the University of Arizona as a Professor. In 2002 he joined the Chitose Institute of Science and Technology as a Professor. He has authored or coauthored more than 225 refereed journal publications, 25 review papers, and 7 textbooks in physics.

and 7 textbooks in physics.



J.-H. Huh received the Ph. D. degree in Chemistry from Myongji University, South Korea, in February 2005. From middle of 2005, he was a Postdoctoral Researcher in the Coatings & Polymeric Materials Department of North Dakota State University, Fargo, USA. At the end of 2007, he joined Professor Ikuo Suemune's group, Research Institute for Electronic Science, Hokkaido University, Japan, as Postdoctoral Researcher. His current research is focused on new emitting devices development for

single (entangled) photon sources.



Claus Hermannstädtter born in 1979, studied Physics at the University of Stuttgart, Germany, where he obtained his Diplome in 2006 and Ph. D. in 2009 with Honors. From 2006 to 2010 he conducted research in the fields of semiconductor nanostructures and quantum optics, especially focusing on coupled quantum dots. Being awarded a JSPS Scholarship for Foreign Researches, he joined Professor Ikuo Suemune's group at Hokkaido University, Japan, in May 2010. His current

research interests are quantum dot based telecom wavelength single and entangled photon emitters and quantum devices, as well as novel semiconductor-superconductor hybrid devices.



Satoru Odashima received his B.S. from Tokyo University of Science in 1991, his M.S. from Tohoku University in 1993, and his Dr. E. from Iwate University in 2000. He is currently engaged in research on highly correlated electron systems (particularly transition-metal oxides) and semiconducting materials. He is a member of the Physical Society of Japan, the Japan Society of Applied Physics, and the Information Processing Society of Japan.



Hidekazu Kumano received his M.S. degree in Science from the Hokkaido University, Japan, in 1996. He received the degree of Doctor (Engineering) from the Hokkaido University, Japan, in 2004. He is an Associate Professor of the Research Institute for Electronic Science (RIES) of the Hokkaido University from 2007. His recent research interests are in the area of quantum information science and the physics of low-dimensional semiconductors especially photon-electron mutual conversion.

electron mutual conversion.